Numerical analysis of centrifugal water pump impeller under varying loads

L Yadeta[1,*] H G Lemu[2] and Addisu K/Mariam Tadese [1]

[1] Jimma Institute of Technology, Jimma University, Ethiopia
[2] Faculty of Science and Technology, University of Stavanger, Stavanger, Norway

[*] Corresponding author's e-mail: letamchengrju@gmail.com

Abstract. Centrifugal pumps are widely used to move liquids from one place to another at varying pressure and flow rate, and to an elevated height for irrigation, water supply plants, and steam power plants. The load variations often lead to unpredictable performance of the impeller. The objective of this study is to investigate the performance of a three-stage centrifugal water pump impeller under varying loads using numerical methods. To conduct the investigation, a water pump used by Jimma town water treatment station, which operates with head of 191 m and discharges 439.2 m3/hr water was used as a case study. Computational fluid dynamics analysis of the pump was conducted using ANSYS 19.0 CFX to get the pressure distribution at different flow rates (60%, 100% and 140% of the design flow rate). The fluid pressure was then used to make static stress analysis of the impeller employing one way fluid structural interaction analysis for three different materials. The finding of the study shows that the fluid pressure on the impeller has great impact on the impeller performance causing high stress and deformation of the impeller.

Keywords: Centrifugal pump, computational fluid dynamics, fluid-structure interaction, Navier Stokes equation, numerical analysis

1. Introduction

Pump is a mechanical device that applies energy to move liquids from one place to another at increased pressure, flow rate and to an elevated height. Irrigation, fire-fighting services employ pumps of different sizes [1]. Pumps and turbo-pumps are used in many technological areas and cover a wide range of applications such as thermal power generation, nuclear, propulsion, marine and water supply [2]. The pumps can be divided into two general categories, namely dynamic pumps and displacement pumps. In a dynamic pump, such as a centrifugal pump, energy is added to the pumping medium continuously and the medium is not contained in a set volume. The energy, in a displacement pump such as a diaphragm pump, is added to the pumping medium periodically while the medium is contained in a set volume. The pump is driven by a prime mover that is either an engine or an electric motor. The capacity of a pump is defined based on the pressure head (in meters) and the maximum delivery flow rate at a specific speed of the shaft [3]. Centrifugal pumps are one of the dynamic pumps which consists of a set of rotating vanes enclosed within a casing and is used to impart energy to a fluid through centrifugal force. Centrifugal pump is a device mainly used for transporting liquid from lower level to higher level. Centrifugal pumps convert mechanical energy from a motor to energy of a moving fluid, where some of the energy goes into kinetic energy of fluid motion, and the rest is converted to potential energy that is represented by a fluid pressure or by lifting the fluid against gravity to a higher level [4][5].

Centrifugal pumps are widely used for irrigation, water supply plants, steam power plants, sewage, oil refineries, chemical plants, hydraulic power service, food processing factories and mines, because of their suitability in practically any service. In pumps the mechanical energy is converted into hydraulic energy [6]. The two main components of centrifugal pump are impeller and casing. Centrifugal pump moves liquid by rotating one or more impellers inside a volute casing. The liquid is introduced through the casing inlet to the eye of the impeller where it is picked up by the impeller vanes. The rotation of the impeller at high speeds creates the centrifugal force that

throws the liquid along the vanes, causing it to be discharged from it's out-side diameter at a higher velocity. This velocity energy is converted to pressure energy by the volute casing prior to discharging the liquid to the system [7]. The second part of centrifugal pump is stationary element comprising the casing, bearings and seals. A shaft is used to support rotating components or to transmit power or motion by rotary or axial movement [7]. Mechanical component fails due to either a decrease in its strength or an increase in load acting on it. Failure of a component affects the performance of a pump, causing either a reduction in its efficiency or its complete breakdown. In industrial applications, the probability of occurrence of critical problems such as component damage and pump failure is high due to heavy loads and the demand for continuous operation of the pump. In such cases, the entire plant will have to be shut down until the pump is either brought back to service or replaced. In order to prevent huge economic losses incurred due to such a shut-down, a pump must function reliably under specified operating conditions [8]. Centrifugal water pump components are subjected to different loading conditions. It is also subjected to corrosion and corrosion assisted fatigue due to the operating or working environment. In order to perform numerical analysis of centrifugal pump impeller, numerical calculations were performed by solving the 3D Navier-Stoke´s and energy equations using the commercial code ANSYS CFX [9]. In the same study, steady-state analysis was performed using the κ-ω based shear stress transport (SST) model, which proved to give relatively accurate predictions in fluid machine analysis. Using an FSI analysis, it is possible to see the Coriolis forces and centrifugal forces generated by the impeller. FSI analysis is a multiphysics interaction between fluid flow and a solid structure. There are two ways to do an FSI analysis (1) one-way coupling and (2) two-way coupling. Benra et al. [10] employed one-way FSI coupling, in which the CFD results were transferred to the structural analysis, while in two-way FSI, the deformations in the structure obtained from the transfer of the CFD results are fed back to the CFD environment. The objective was to determine the deviation in the flow created as a result of the structural deformation. The study by Gu et al. [11] demonstrated the effect of FSI on rotational forces. The study indicated that fluid pressures significantly affect von-Mises stress. Kobayashi et al. [12] investigated a mixed-flow pump with an unshrouded impeller by one-way coupled FSI, and the distribution of stress on the impeller was obtained. Piperno et al. [13] concluded that to ensure the safe operation of a rotating structure for every flow rate, the analysis of stress and deformation on the impeller in the unstable operation region needs to be solved by the consideration of FSI. Kang and Kim [14] pointed out that structural safety needs to be evaluated because the impeller receives fluid pressure load and centrifugal force during the operation. Even though different researches were conducted, many of them focused on centrifugal compressor impellers and less study was conducted on the FSI stress analysis of centrifugal pump impeller. This study focuses on one-way FSI stress analysis of three stage centrifugal water pump impeller. It is case study of Jimma town water treatment station, which is located at Boye and pumps water with head of 191 m and 439.2 m^3/hr discharges.

2. Methodology

Actual design data about the specification of a given centrifugal water pump was collected from the Jimma town water treatment station located at Boye. Based on the collected data, the 3D model of the centrifugal water pump shaft, impeller and return guide vane was prepared by using ANSY 19.0 geometry modelling and SolidWorks modelling software. Impeller was modelled using Vista CPD Design to model impeller blades from 1D to 3D geometry.

In this study based on recommended number of impeller, in this study six blades impellers were chosen. In this study Complex 3-D Computational Fluid Dynamics analysis was performed to get the pressure distribution of the impellers by using ANSYS 19.0 software. ANSYS CFX was used to perform steady state CFD analysis of the three-stage centrifugal pump. One-way partitioned FSI analysis was used to determine the stress of the three-stage pump where the fluid pressure on the structure will be transferred to the solid solver. The fluid flow is modelled as incompressible flow using water as a working fluid. k-SST omega turbulence model was used by considering wall of solid is modelled as no-slip condition.

The principles of conservation law governed by fluid dynamics are[15]:

$$\frac{\partial u_i}{\partial x_i} = 0 \tag{1}$$

$$\rho\left(\frac{\partial u_i}{\partial t} + u_j \frac{\partial u_i}{\partial x_j}\right) = -\frac{\partial p}{\partial x_j} + \frac{\partial}{\partial x_j}\left(\mu \frac{\partial u_i}{\partial x_j} - \overline{\rho \acute{u}_\iota \acute{u}_j}\right) \tag{2}$$

Where u_i is velocity vector, p is pressure scalar, ρ is density, i and j is tension notations, $\overline{\rho \acute{u}_\iota \acute{u}_j}$ is apparent stress turbulence tensor, μ is the dynamic viscosity. The $k-\omega$ based SST model accounts for transport of turbulence shear stress and highly accurate prediction of the onset of the amount flow separation under adverse

pressure gradients. The unknown turbulent viscosity μ_t is determined by solving two additional transport equations for turbulent energy k and for the turbulence frequency ω. These two equations can be written as:

$$\frac{\partial(\rho\kappa)}{\partial t} + \frac{\partial}{\partial x_j}(\rho k u_j) = \frac{\partial}{\partial x_j}[(\mu + \frac{\mu_t}{\sigma_k})\frac{\partial k}{\partial x_j}] + p_k - \beta_{\rho k\omega}' + p_k b \quad (3)$$

$$\frac{\partial(\rho\omega)}{\partial t} + \frac{\partial}{\partial x_j}(\rho\omega . u_j) = \frac{\partial}{\partial x_j}[(\mu + \frac{\mu_t}{\sigma_\omega})\frac{\partial\omega}{\partial x_j}] + \alpha\frac{\omega}{\kappa}p_k - \beta_{\rho\omega^2} + p_k b \quad (4)$$

The impeller is modelled in the blade frame, and the diffuser and return guide vane is in the fixed frame of the reference and both of them are related each other through the frozen rotor. The boundary conditions given in Table 1 were applied:

Table 1. CFD simulation boundary conditions

Boundary condition	Value
Working fluid	Water
Temperature	25 ^{0}C
Inlet pressure	0.3 bar
Speed	1480 rpm
Turbulence intensity	5%
Discharge flow rate	73.2 kg/s, 122 kg/s, 170.8 kg/s
Turbulence model	κ-ω SST

To simulate the pump under different flow rate operating conditions, the outlet mass flow rate was set to flow rates 0.6 Qd = 73.2 kg/s, Qd = 122 kg/s and 1.4 Qd = 170.8 kg/s design flow rate. Three dimensional incompressible Navier Stokes equations were solved with ANSYS 19.0-CFX Solver. In addition, a no-slip flow condition is applied on the walls (on the blade, hub and shroud). Smooth wall function was selected.

Unstructured meshes in CFX meshing was used to reduce the amount of time spent generating meshes, simplifying the geometry modeling and mesh generation process. Apart from its higher memory requirement unstructured mesh is also preferable for complex geometry. In this study unstructured mesh tetrahedral cells were used because the fluid domain in the pump has complex geometry. The geometry and the mesh of a six bladed pump impeller and diffuser with return guide vane domain were generated with CFX meshing as shown in Figure 1(a)-(d). Un- structured meshes with tetrahedral cells were used for the domain of impeller and diffuser with return guide vane as well as for the inlet and out- let casing of fluid domain.

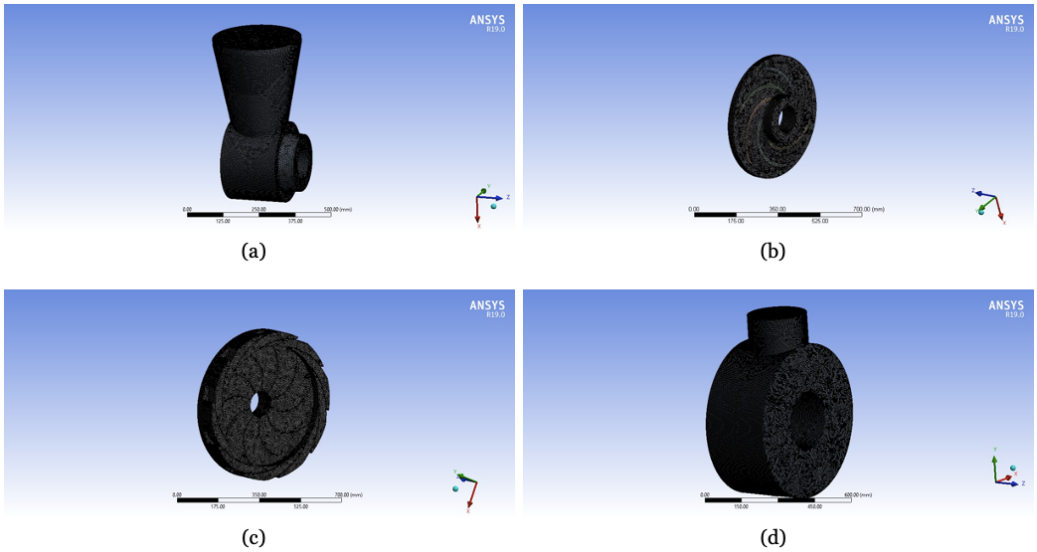

Figure 1. CFD Fluid domain mesh

To assure accuracy of simulation mesh independence in the flow domain must be determined before starting the CFD studies. In this study, the calculation domain was divided into unstructured grids by CFX Meshing. Seven mesh element size with the same numerical settings were analyzed to select appropriate mesh number of elements to carry out the CFD analysis of three stage centrifugal pump. As it can be observed from Figure 2 grid size minimally influences the numerical results, and the overall difference is within 1%. So, for the analysis of the three-stage centrifugal pump 2 353 607 elements were selected considering time and computational cost.

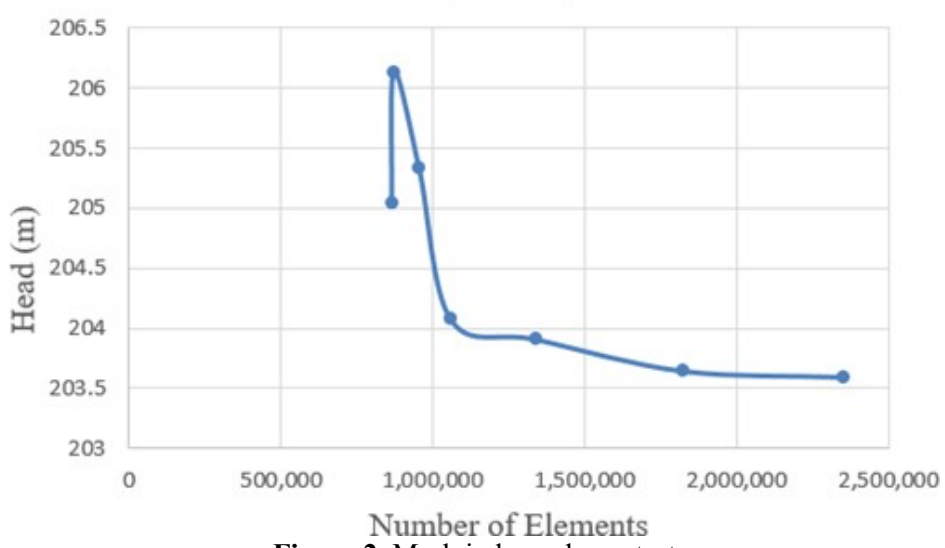

Figure 2. Mesh independency test

For centrifugal pump impeller the following materials was selected. Pump impeller operates in corrosive environment. The three selected material for impeller stress analysis are G-Cu-Sn10 Copper Tin Alloy, EN-GJL-250 Grey Cast Iron and G-X6CrNiMo18-10 stain- less steel.

3. Discussion of results

With the aid of CFD, the complex internal flow in the three stage centrifugal pump was predicted quite well. In this study, a steady state solution with κ-ω SST turbulence model was used in ANSYS-CFX for analysis of three stage centrifugal pump CFD simulation. From the manufacturers experience pumps may operate other than BEP of the pump which operates at nominal operating conditions. In this study the analysis of three stage centrifugal pump at off design condition was carried out at different flow rates 60% Qd, Qd and 140% Qd design flow rate. The analysis of the three-stage pump at different flow rate was carried out to see the impact of different flow condition on stress performance of an impellers. The CFD simulation result of the pump is shown in Figure 3 below.

The total head of the pump at the design flow rate of 439.2 m^3/hr obtained from the CFD analysis of the three-stage pump is 203.597 m. The head rise obtained through CFD analysis was over predicted the head rise than the design head of the pump which was 191 m. The over prediction of the CFD result is because leakage was not considered due to its computational cost and complexity in CFD simulation, additionally surface roughness of impeller, diffuser with return guide vanes was assumed to be smooth which in turn increases head of CFD when neglected. Figure 3 shows CFX simulation result of flow rate versus head. As it can be observed from Figure 3 as the flow rate increases the head of the pump decreases and vice versa.

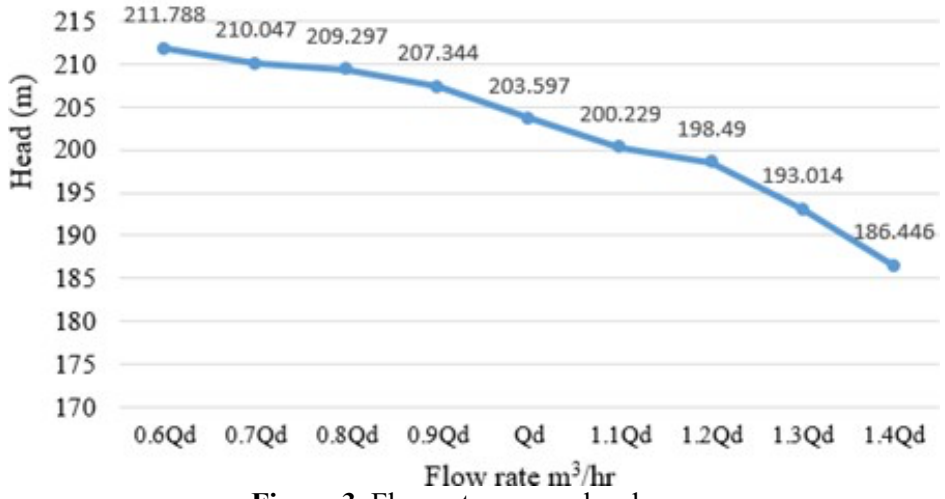

Figure 3. Flow rates versus head

3.1 Pressure distribution

From CFD simulation of the pump pressure distribution of the pump was obtained. Total pressure on pressure side of the blade is more than that of suction side. The difference of pressure from the pressure side to the suction side of the impeller blade is increasing from leading edge to trailing edge of the blade. The total pressure patterns are varying along the span of the impeller. Low total pressures are observed near hub of the impeller. Figure 4 shows pressure distribution of the CFD simulation of the pump at design flow rate $Qd = 439.2\ m^3/h$. The pressure rise increases from the first stage impeller to the subsequent stage impellers of the pump.

As it can be observed from Figure 4(a), the maximum total pressure for the first stage impeller at design flow rate (Qd) is 0.6962 MPa and the minimum total pressure is -0.181 MPa. Similarly, as it is shown in the Figure 4(b) and (c) maximum pressure of second and third stage impeller is 1.330 MPa and 1.916 MPa respectively while minimum total pressure is 0.5127 MPa and 1.150 MPa. As it is indicated in Table 2, for 0.6Qd flow rate the maximum total pressure for the first stage impeller is 0.7633 MPa and the minimum total pressure is -0.09933 MPa. Similarly, the maximum pressure of second and third stage are 1.386 MPa and 1.973 MPa respectively while the minimum total pressure of second and third stage is 0.5365 MPa and 1.155 MPa respectively.

For 1.4Qd flow rate (Table 2), the maximum total pressure for the first stage impeller is 0.6686 MPa and the minimum total pressure is -0.1267 MPa. Similarly, the maximum pressure of the second and third stage impellers are 1.261 MPa and 1.794 MPa respectively, while the minimum total pressure of second and third stage is 0.5154 MPa and 1.096 MPa respectively. Generally, as it can be observed from Table 2, at different flow rates of the pump, the pressure of the fluid increases as the fluid flows from the suction side to the discharge side at each stage of the pump. In all operating conditions, the global maximum pressure was observed at the third stage impeller. Additionally, the pressure of the pump decreases as the flow rate of the pump increases and vice versa.

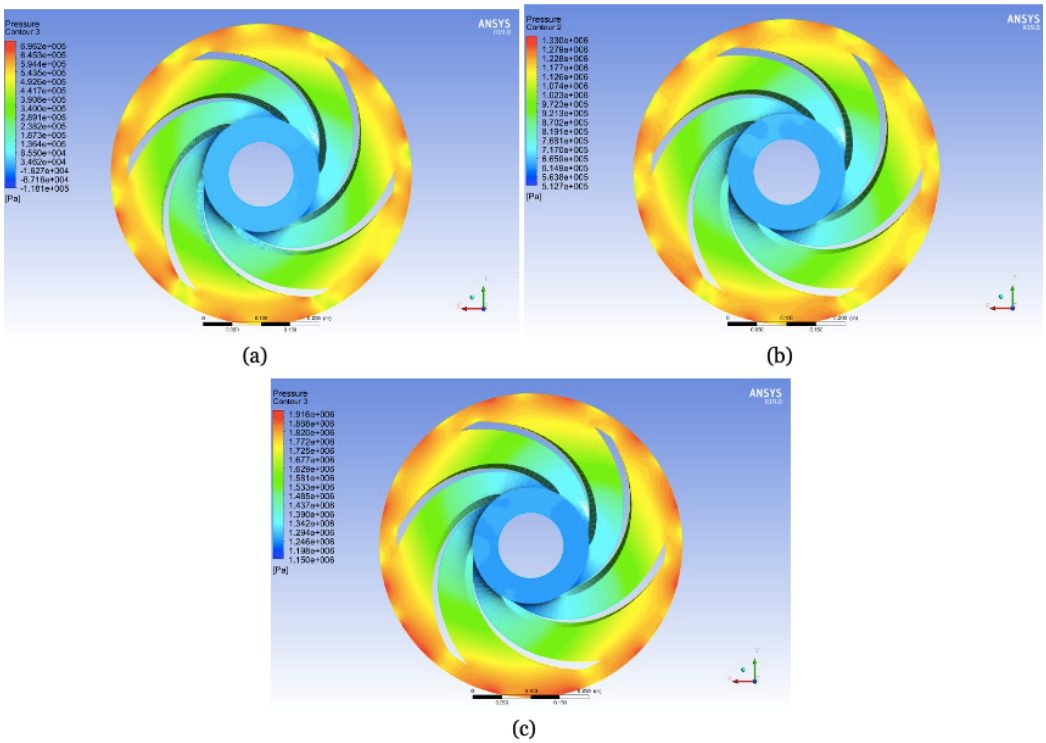

Figure 4. Pressure distribution in impeller (a) Stage I (b) Stage II (c) Stage III

Table 2. Pressure distribution

Flow Rate (m^3/hr)	Pressure distribution (MPa)					
	Stage I		Stage II		Stage III	
	Max	Min	Max	Min	Max	Min
0.6Qd	0.7633	-0.099331	1.386	0.5365	1.973	1.155
Qd	0.6962	-0.1181	1.330	0.5127	1.916	1.150
1.4Qd	0.6686	-0.1267	1.261	0.5154	1.794	1.096

3.2 FSI stress analysis in the impeller

Numerical stress analysis of the impellers of the three-stage centrifugal water pump was performed. The pressure distribution on the surface of the impeller was imported to FEA module to perform FSI stress analysis of the impeller at 0.6Qd, Qd and 1.4Qd flow rates of the pump operation. In this study, factor of safety was analyzed only for the third stage impeller because the third stage impeller experiences maximum pressure in all flow rate conditions which leads to higher stress and deformation.

3.2.1 FSI stress analysis at 0.6Qd flow rate: FSI stress analysis was analyzed at 0.6Qd flow rate of the pump operation for three different materials. In the first stage impeller, maximum equivalent stress for G-Cu-Sn10 Copper Tin Alloy is 50.521 MPa and minimum equivalent stress is 0.00399 MPa (Table 3). The data in the table also shows that FSI stress analysis result for EN-GJL-250 Grey Cast Iron and G-X6CrNiMo18-10 impeller materials is 49.676 MPa and 50.057 MPa respectively. Similarly minimum equivalent stress for both material is 0.0044873 MPa and 0.0052831 MPa.

Table 3. FSI equivalent stress of impeller at 0.6Qd flow rate

Materials	Equivalent stress (MPa)					
	Stage I		Stage II		Stage III	
	Max	Min	Max	Min	Max	Min
G-Cu-Sn10 Copper Tin Alloy	50.521	0.00399	110.61	0.094794	171.32	0.10044
EN-GJL-250 Grey Cast Iron	49.676	0.0044873	108.33	0.083661	167.72	0.12008
G-X6CrNiMo18-10	50.057	0.0052831	109.36	0.0720061	169.4	0.088268

As the pressure of water increases from first stage to the second stage, it is expected that equivalent stress of the second stage increases. As it can be observed from Table 2, the maximum equivalent stress of the second stage impeller of the pump is for G-Cu-Sn10 Copper Tin Alloy is 110.61 MPa and minimum equivalent stress is 0.094794 MPa. Similarly maximum equivalent stress of the second stage impeller for EN-GJL-250 Grey Cast Iron and G-X6CrNiMo18-10 is 108.33 MPa and 109.36 MPa respectively. Additionally, minimum equivalent stress for both materials are 0.083661 MPa and 0.0720061 MPa respectively.

Generally, as it can be observed that the stress in the impeller increases from the first stage to the third stage because as the number of stages of the impeller increases, the pressure of the water rises which results in high pressure on the surface of the impeller as the pump stage increases. It can be concluded that the third stage impeller is critical impeller as it experiences high stress.

3.2.2 FSI stress analysis at Qd flow rate: This section discusses results of FSI stress analysis in the impeller at design flow rate operation of the pump. Like previous case, FSI stress analysis was performed for three different materials of the impeller. Results obtained from the analysis are illustrated in Figure 5 and summarized in Table 4. As it is shown in the table, for first stage impeller, maximum equivalent stress for G-Cu-Sn10 Copper Tin Alloy is 50.802 MPa and minimum equivalent stress is 0.018 MPa. Similarly, maximum equivalent stress of the first stage impeller for EN-GJL-250 Grey Cast Iron and G-X6CrNiMo18-10 is 48.1 MPa and 48.51 MPa respectively. Additionally, minimum equivalent stress for both materials is 0.025 MPa and 0.013 MPa. From second stage impeller, FSI stress analysis for G-Cu-Sn10 Copper Tin Alloy maximum equivalent stress is 108.98 MPa while minimum equivalent stress is 0.128. Similarly, as it is shown in Table 4, maximum equivalent stress of the second stage impeller for EN- GJL-250 Grey Cast Iron and G-X6CrNiMo18- 10 is 105.93 MPa and 107.05 MPa respectively.

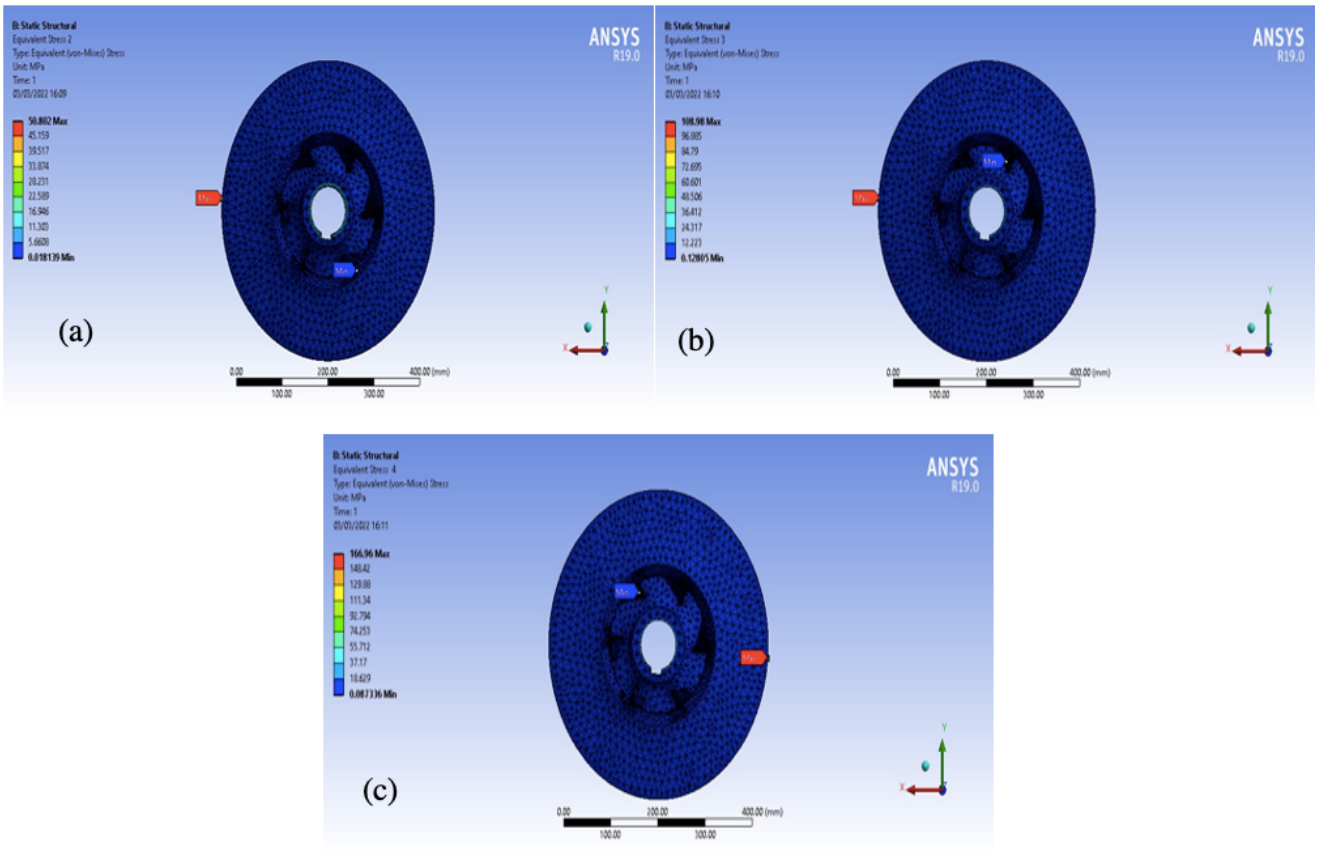

Figure 5. Equivalent stress for G-Cu-Sn10 Qd flow rate (a) Stage I (b) Stage II (c) Stage III.

Also, minimum equivalent stress for both material is 0.094 MPa and 0.115 MPa respectively. Compared to first stage impeller, the equivalent stress for the three materials has been increased. In the case of third stage impeller FSI stress analysis, equivalent stress increased for all the three materials as compared to the first and second stage impeller. As it can be observed from Table 4, the maximum equivalent stress of the third stage impeller of the pump for G-Cu-Sn10 Copper Tin Alloy is 166.96 MPa and minimum equivalent stress is 0.087 MPa. Similarly maximum equivalent stress of the third stage impeller for EN-GJL-250 Grey Cast Iron and G-X6CrNiMo18-10 is 161.34 MPa and 163.05 MPa respectively. Additionally, minimum equivalent stresses for both materials are 0.12671 MPa and 0.10297 MPa respectively. Generally, the stress in the impeller increases from the first stage to the third stage because the pressure of the water rises as the pump stage increases, which results in high pressure on the surface of the impeller.

Table 4. FSI equivalent stress of impeller at Qd flow rate

Materials	Equivalent stress (MPa)					
	Stage I		Stage II		Stage III	
	Max	Min	Max	Min	Max	Min
G-Cu-Sn10 Copper Tin Alloy	50.802	0.018	108.98	0.128	166.96	0.087
EN-GJL-250 Grey Cast Iron	48.097	0.025	105.93	0.094	161.34	0.127
G-X6CrNiMo18-10	48.509	0.013	107.05	0.115	163.05	0.103

3.2.3 FSI impeller equivalent stress at1.4Qd flow rate: The FSI stress analysis results for three stage impeller is presented in Table 5. As shown, maximum equivalent stress of the first stage impeller of the pump for G-Cu-Sn10 Copper Tin Alloy is 49.251 MPa and minimum equivalent stress is 0.012 MPa. Similarly maximum equivalent stress of the first stage impeller for EN-GJL-250 Grey Cast Iron and G-X6CrNiMo18-10 stainless steel are 48.366 MPa and 48.764 MPa respectively. Also, the minimum equivalent stress for both materials are 0.0174 MPa and 0.020 MPa respectively.

On the other hand, the equivalent stress in the second stage impeller for G-Cu-Sn10 Copper Tin Alloy is 103.96 MPa and minimum equivalent stress is 0.096 MPa. Similarly, as it can be observed from Table 5 that maximum equivalent stresses of the second stage impeller for EN-GJL-250 Grey Cast Iron and G- X6CrNiMo18-10 are 101.78 MPa and 102.78 MPa respectively. Additionally, minimum equivalent stresses for both materials are 0.0476 MPa and 0.092 MPa.

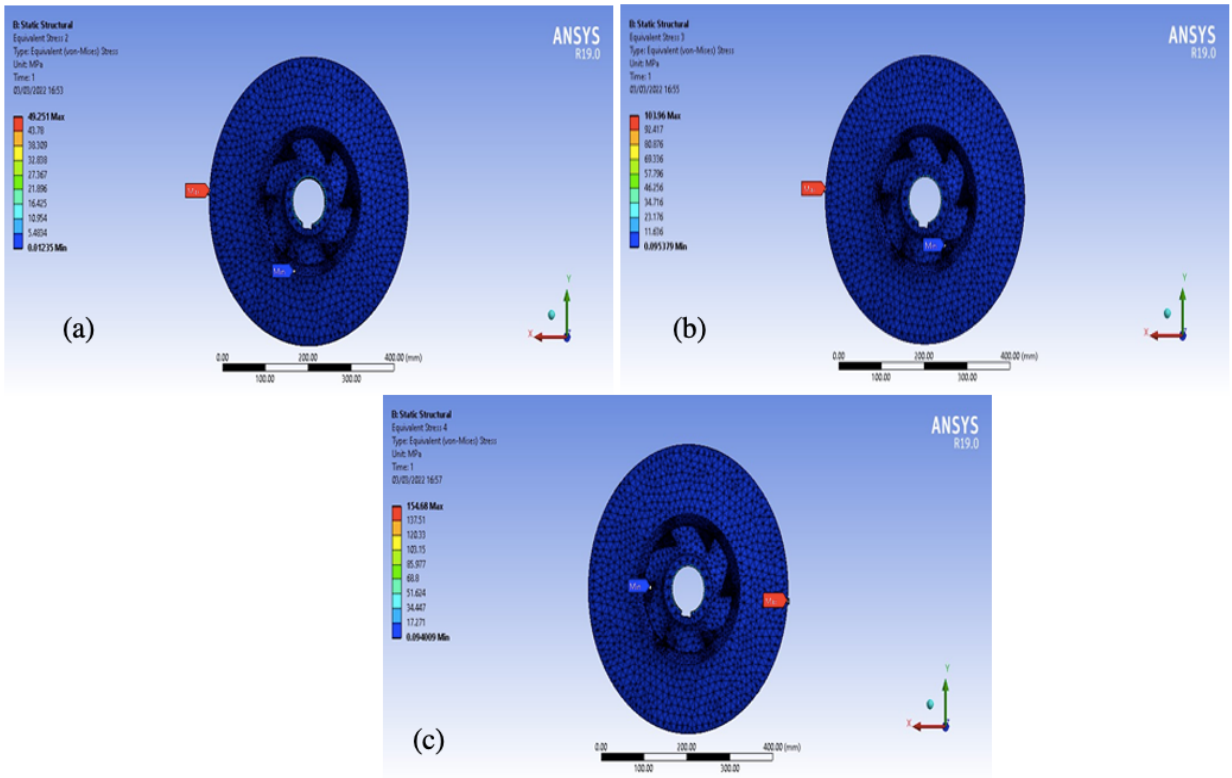

Figure 6. Equivalent stress for G-Cu-Sn10 Qd flow rate (a) Stage I (b) Stage II (c) Stage III.

At 1.4Qd flow rate operation of the pump, the equivalent stress at third stage is greater than that of the first two stage impellers. As it can be observed from Table 5, maximum equivalent stress of third stage impeller of the pump for G-Cu-Sn10 Copper Tin Alloy is 154.68 MPa and minimum equivalent stress is 0.094 MPa. Similarly, as it indicated in Table 4.20 maxi- mum equivalent stress of the third stage impeller for EN-GJL-250 Grey Cast Iron and G- X6CrNiMo18-10 is 151.21 MPa and 152.86 MPa respectively. Also minimum equivalent stress for both material is 0.122 MPa and 0.076 MPa. Generally, the stress of the impeller increases from the first stage to the third stage because of the fact that as the stage of the impeller increases the pressure of the water rise which results in high pressure on the surface of the impeller as the pump stage increases.

The study shows that in all operating conditions of the pump minimum stress was observed near the hub on the suction side of the pump. Research indicated that in centrifugal pump impellers, the minimum pressure exists at the suction side of the impeller. The lowest result of pressure at the suction side of the impeller results in the lowest equivalent stress value at the suction side of the impeller. As it can be observed from the above stress analysis of the impeller at all flow rate conditions i.e at 60%Qd, Qd and 1.4 Qd flow rate the maximum equivalent stress was observed on the pressure side at the trailing edge of the pump. The result agrees with previous research conducted [16].

Table 5. FSI equivalent stress of impeller at 1.4Qd flow rate

Materials	Equivalent stress (MPa)					
	Stage I		Stage II		Stage III	
	Max	Min	Max	Min	Max	Min
G-Cu-Sn10 Copper Tin Alloy	49.251	0.012	103.96	0.095	154.68	0.094
EN-GJL-250 Grey Cast Iron	48.366	0.017	101.78	0.048	151.21	0.122
G-X6CrNiMo18-10	48.764	0.020	102.78	0.091	152.86	0.076

3.3 FSI Total deformation of impeller

3.3.1 FSI Total deformation of impeller at 0.6Qd flow rate: From FSI stress analysis of impeller total deformation of impeller at different stages of the pump was carried out. In this study total deformation analysis was carried out only for the third impeller because third stage impeller experiences high pressure and stress. Maximum total deformation of third stage impeller of the pump for G-Cu-Sn10 Copper Tin Alloy is 1.4609 mm and minimum total deformation is 0.037053 mm. Similarly total deformation of the third stage impeller for EN-GJL- 250 Grey Cast Iron and G-X6CrNiMo18-10 is 1.5 mm and 1.3959 mm respectively. Additionally, minimum deformation for both material is 0.035975 mm and 0.038336 mm.

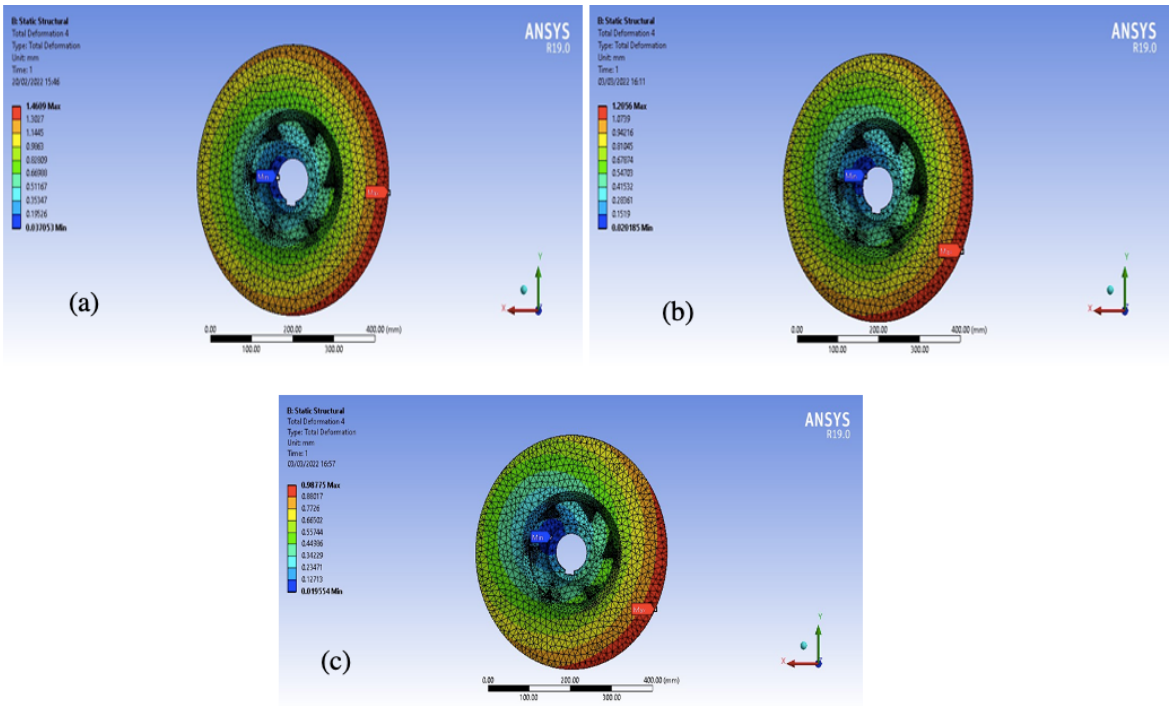

Figure 7. Total deformation for G-Cu-Sn10 impeller material at (a) 0.6Qd flow rate, (b) Qd flow rate and (c) 1.4Qd flow rate

Table 6. FSI Equivalent stress of impeller at 0.6Qd, Qd and 1.4Qd flow rate

Materials	Total deformation (mm)					
	0.6Qd		Qd		1.4Qd	
	Max	Min	Max	Min	Max	Min
G-Cu-Sn10 Copper Tin Alloy	1.4609	0.037053	1.2056	0.020185	1.4661	0.037053
EN-GJL-250 Grey Cast Iron	1.5	0.035975	1.2556	0.021183	1.5	0.019502
G-X6CrNiMo18-10	1.3959	0.038336	1.2065	0.020871	1.4425	0.01894

3.3.2 FSI Impeller total deformation at Qd flow rate: As it can be observed from Table 3 above the maximum total deformation of third stage impeller of the pump for G-Cu-Sn10 Copper Tin Alloy is 1.2056 mm and minimum total deformation is 0.020185 mm. Similarly, from Table 4.19 total deformation of the third stage impeller for EN-GJL-250 Grey Cast Iron and G-X6CrNiMo18-10 Stain- less steel is 1.2556 mm and 1.2065 mm respectively. Additionally, minimum total deformation for both material is 0.021183 mm and 0.020871 mm respectively.

3.3.3 FSI impeller total deformation at 1.4Qd flow rate. Total deformation of the third stage impeller at 1.4Qd flow rate of the pump discussed. Results obtained from total deformation is presented in Table 3 above. As it can be observed from the Figure 7 maximum total deformation of third stage impeller of the pump is for G-Cu-Sn10 Copper Tin Alloy is 1.46609 mm and minimum deformation is 0.037053 mm. Similarly total deformation of the third stage impeller for EN-GJL-250 Grey Cast Iron and G- X6CrNiMo18-10 is 1.5 mm and 1.4425 mm respectively. Also, minimum total deformation for both material is 0.019502 mm and 0.01894 mm. In all cases

of the operating conditions of the pump maximum impeller deformation was observed at the trailing edge of the impellers in all the three materials of the pump. This is due to the fact that the pressure inside the impeller increases from the leading edge of the pump to the trailing edge of the pump hence it creates high stress and deformation at the trailing edge of the impeller of the pump.

3.4 FSI safety factor of impeller at different flow rate:

Stage III FSI safety factor at 0.6Qd flow rate: In this study, the safety factors were analysed only for the third stage impeller. This is due to the fact that the impellers have the same geometry, and from the three impellers arranged in series on the shaft, the third stage impeller experiences high stress and deformation. As it can be observed from Figure 8(a), the safety factor at 0.6Qd flow rate of the pump for G-Cu- Sn10 Copper Tin Alloy is around 0.76, while for EN-GJL- 250 Grey Cast Iron and G-X6CrNiMo18-10, the safety factors 0.98 and 1.24 respectively. Factor of safety for G-Cu-Sn10 Cop- per Tin Alloy and EN-GJL-250 Grey Cast Iron is less than one which means the impeller fail be- fore design life of the impeller. Factor of safety for G-X6CrNiMo18-10 is 1.24 which indicates that the impeller is safe because the safety factor is greater than one.

Stage III FSI safety factor at Qd flow rate: As it can be observed from the Figure 8(b), the safety factor for G-Cu-Sn10 Copper Tin Alloy is around 0.78, while for EN- GJL-250 Grey Cast Iron and G-X6CrNiMo18-10 the safety factors are 1.02 and 1.3 respectively. Factor of safety for G-Cu-Sn10 Cop- per Tin Alloy is less than one, which means the impeller fails before its design life. The safety factor for G-X6CrNiMo18-10 is 1.29 which is also greater than one implying that the impeller is safe.

Stage III FSI safety factor at 1.4Qd flow rate: Plot of the safety factor distribution for this case is given in Figure 8(c), where it is observed that the value for G- Cu-Sn10 Copper Tin Alloy is 0.76. For EN-GJL-250 Grey Cast Iron and G-X6CrNiMo18-10, the minimum safety factor values are 0.98 and 1.24 respectively. It indicates that the safety factor for G-Cu-Sn10 Copper Tin Alloy and EN-GJL-250 Grey Cast Iron are less than one, which means the impeller fails before its design life. On the other hand, the G-X6CrNiMo18-10 material is safe because its safety factor is 1.24 which is greater than one.

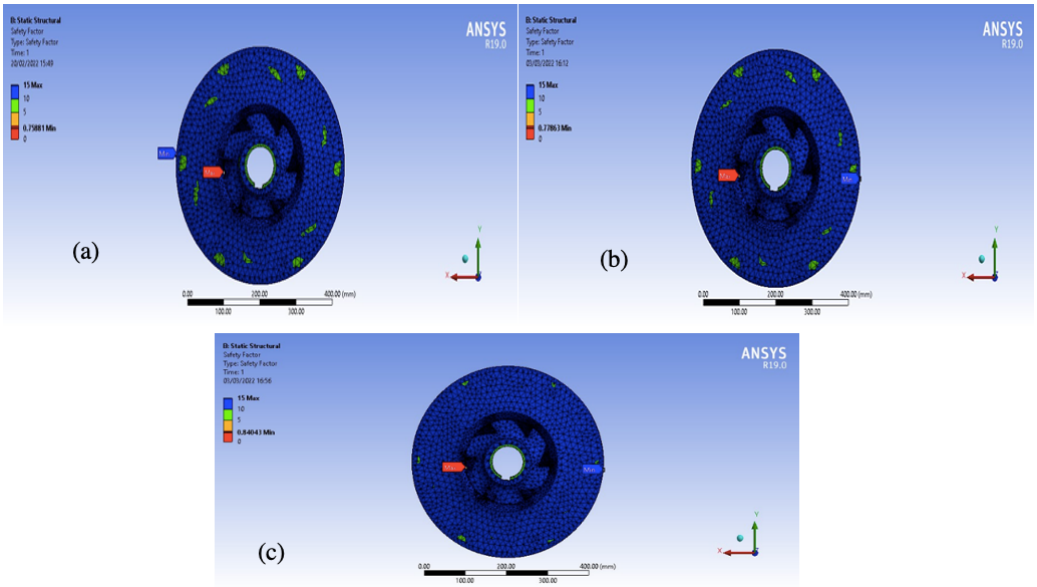

Figure 8. Stage III safety factor for G-Cu-Sn10 impeller material at (a) 0.6Qd flow rate, (b) Qd flow rate and (c) 1.4Qd flow rate

4. Conclusion

To investigate the effect of the fluid pressure on centrifugal water pump impeller, CFD analysis of a three-stage centrifugal pump was carried out using ANSYSS CFX at different flow rates of the pump ranging from 0.6Qd to 1.4Qd flow rates. In the analysis, a steady state solution with k- SST turbulence model was used in ANSYS-CFX for analysis of the centrifugal water pump. The result shows that as the flow rate increases the head of the pump

decreases and as the flow rate of the pump decreases the head developed by the pump increases. The head rise obtained through CFD analysis was over predicted head rise than the design head of the pump which was 191 m. This is due to the fact that leakage was neglected in the analysis of the pump during the analysis and also surface roughness of the impeller, diffuser with return guide vanes was assumed to be smooth.

Numerical stress analysis of the impellers of the three-stage centrifugal water pump was performed, in which it was observed that the pressure distribution on the surface of the impeller varied from suction side to the pressure side of the impeller. The pressure of the fluid does not only vary along the surface of the impeller but also it varies along different stages of the pump. From the finding of the study, the third stage experiences higher deformation and stress than the first and the second stage impeller. The results obtained from the impeller analysis shows that the impeller stress increases as the flow rate decreases because the pressure acting on the wall of the impeller increases as the pump flow rate decreases.

References

[1] Cherkassy V M, Pumps, Fans, Compressor, Mir publishers, 1985.

[2] Benturki M, Dizene R, Ghenaiet A 2018 Multiobjective optimization of two-stage centrifugal pump using NSGA-ii algorithm, *J. Appl. Fluid Mech.* **11**(4) 929- 943.

[3] Khaing C C, Lynn A Z, Nyi N 2019 Design of multistage centrifugal pump impeller for high head applications, *Int. J. Latest Technol. Eng., Manage. Appl. Sci. (IJLTEMAS)* **8**, 115-120.

[4] Rajanand M P 2016 Design & analysis of centrifugal pump impeller by FEA, *Int. Res. J. Eng. Technol. (IRJET),* **03**, 420-428.

[5] Iratkar G G, Gandigude A U 2017 Structural analysis, material optimization using FEA and experimentation of centrifugal pump impeller. *Int. J. Adv. Res. Ideas. Innov. Technol.*, **3**(4), 97-105.

[6] Singh V R, Zinzuvadia M, Sheth S M 2017 Parametric study and design optimization of centrifugal pump impeller-a review, *Int J Eng Res Appl.* **1**, 507-515.

[7] Tamin M N, Hamzah M A 2017 Fatigue failure analysis of a centrifugal pump shaft, In: *Fail. Anal. Prev., Ed. Aidy Ali, IntechOpen,* 1-14, Rijeka, Croatia,.

[8] McKee K K, Forbes G L, Mazhar M I, Entwistle R, Howard I M 2011 A review of major centrifugal pump failure modes with application to the water supply and sewerage industries, *In: Asset Manage. Council (ed), ICOMS Asset Manag. Conf.,* May 16 2011. Gold Coast, QLD, Australia.

[9] Bardina J E, Huang P G, Coakley T 1997 Turbulence modeling validation, *28th AIAA Fluid Dynamics Conference, AIAA- 1997-2121*.

[10] Friedrich-Karl B, Hans Josef D, Ji P. Sebastian S, Bo W 2011 A comparison of one-way and two-way coupling methods for numerical analysis of fluid-structure interactions, *J. Appl. Math.*, **2011**, 1-16.

[11] Gu Y, Pei J, Yuan S, Xing L, Stephen C, Zhang F, Wang X 2018 Effects of blade thickness on hydraulic performance and structural dynamic characteristics of high-power coolant pump at overload condition, *Proc. Inst. Mech. Eng., Part A: J. Power Energy,* **232**, 992-1003.

[12] Kobayashi K, Ono S, Harada I, Chiba Y 2010 Numerical analysis of stress on pump blade by one-way coupled fluid-structure simulation. *J. Fluid Sci. Technol.*. **5**, 219–234.

[13] Piperno S, Farhat C, Larrouturou B 1995 Partitioned procedures for the transient solution of coupled aroelastic problems Part I: Model problem, theory and two-dimensional application. *Comput. Methods Appl. Mech. Eng.* **124**, 79–112.

[14] Kang H S. Kim Y J 2016 A study on the multi-objective optimization of impeller for high-power centrifugal compressor. *Int. J. Fluid Mach. Syst.* **9**, 143–149.

[15] Suh S-H, Kyung-Wuk K, Kim H-H, Cho M T, Yoon I S 2015 A study on multistage centrifugal pump performance characteristics for variable speed drive system, *Procedia Eng.* **105**, 270-275.

[16] Ji P, Shouqi Y, Jianping Y 2014 Dynamic stress analysis of sewage centrifugal pump impeller based on two-way coupling method *Chin. J. Mech. Eng.* **27**(2), 369-375.